MRS Communications (2023) 13:812–817

https://doi.org/10.1557/s43579-023-00350-5

MRS Communications

MRS 50th Anniversary Research Letter

Improving environmental stability of MXene films by intercalation of *N*-methylformamide

Akari Seko, Shun Sakaida, Masashi Koyanagi, Yasuaki Okada, and Takeshi Torita, Murata Manufacturing Co., Ltd., 1-10-1 Higashikotari, Nagaokakyo-shi, Kyoto 617-8555, Japan
Mark Anayee, Mikhail Shekhirev, and Yury Gogotsi, A. J. Drexel Nanomaterials Institute and Department of Materials Science and Engineering, Drexel University, Philadelphia, PA 19104, USA

Address all correspondence to Shun Sakaida at **s_sakaida@murata.com** and Yury Gogotsi at **gogotsi@drexel.edu**

(Received 26 November 2022; accepted 23 February 2023; published online: 16 March 2023)

Abstract

MXenes are a large family of two-dimensional nanomaterials with diverse properties and potentials for electronic, photonic, energy storage, and other applications. Due to their hydrophilicity, MXenes capture water from the surrounding environment, which may lead to swelling and degradation of the assembled multi-layer films. Here we demonstrate that intercalation of *N*-methylformamide (NMF) leads to MXene films with improved stability at high temperatures and high humidity through host–guest hydrogen bonding. Due to strong interaction with MXene surface and occupation of the interlayer spacing, NMF mitigates intercalation of water and allows for better retention of electrical conductivity during prolonged use in hot and humid environments.

With growing use of two-dimensional (2D) nanomaterials, considerable attention is being paid to their environmental stability and protection, because nanoparticulate materials are more reactive compared to their bulk counterparts and also adsorb molecules from the environment due to their high specific surface area. Among those important novel nanomaterials are transition metal carbides, nitrides, and carbonitrides known as MXenes, which have many unique properties, such as high electrical conductivity, but may degrade in environment over time.[1] MXenes are represented by the formula $M_{n+1}X_nT_x$, where n is 1–4, M is an early transition metal, X is C and/or N, and T represents surface terminations. MXenes are typically synthesized by selective etching of the A element from layered MAX phase precursors, $M_{n+1}AX_n$, where A is a group 13 or 14 element. After etching in aqueous acidic solution, the exposed transition metal carbide layers are capped with surface terminations (–F, –O, –OH, etc.) from the etching environment. Pristine MXenes and their composites with high electrical conductivities (exceeding 20,000 S cm^{-1}) and high surface areas have been extensively studied for various applications, including energy storage, catalysis, and molecular separation.[2]

The surface terminations render MXenes hydrophilic, which allows them to be easily processed from aqueous suspensions into coatings, fibers, or 3D structures. However, it also poses challenges because of the strong interaction between water and MXenes. In particular, the presence of water near defects, such as metal vacancies, leads to MXene degradation.[3,4] Water attacks MXene nanosheets in aqueous suspensions through hydrolysis reactions, forming transition metal oxides, amorphous carbon, and/or methane gas.[5] Similarly, multilayer MXene assemblies are prone to degradation when they contain water intercalated or adsorbed on their surfaces. MXenes swell similar to aluminosilicate or smectite clay minerals, where multiple layers of water can be incorporated in the interlayer space.[6,7] The presence of water also affects the physicochemical properties, such as the electrical conductivity, which decreases as the lattice expansion leads to decreased interflake contact and diminished electron transport in the out-of-plane direction.[8–10] Therefore, controlling the interaction between MXene and water is important for applications using unprotected MXene-based materials and devices, especially in humid conditions. Significant efforts have been devoted to mitigating swelling through intercalation of multivalent metal ions,[11] encapsulation,[12,13] densification using polymer-based films,[14] thermal crosslinking of layers,[15] and chemical crosslinking with linker molecules.[16]

Because of the oxide/hydroxide-like surfaces of MXenes, hydrogen bonding plays a vital role in the interaction of MXenes with other materials, such as polymers,[17] cellulose,[18] and hydrogels.[19] Hydrogen bonding of MXene layers to oxygen-rich macromolecules is a promising approach to prevent swelling and oxidation.[16] However, the bulky macromolecules used previously may significantly separate MXene layers and reduce the electrical conductivity of the fabricated MXene films. We previously showed that intercalation of hydrazine (N_2H_4) greatly decreased the amount of water between $Ti_3C_2T_x$ MXene layers and had a pillaring effect due to hydrogen bonding.[20] Other molecules, such as formamide (CH_3NO) and its derivatives, are also known for their ability to form hydrogen bonding networks.[21] For example, intercalation of clay materials, such as kaolinite, with *N*-methylformamide (NMF, CH_3NHCHO) led to a decrease in the specific

surface area despite the increase in interlayer spacing, likely because the NMF molecules bridge the adjacent layers through hydrogen bonding.[22] Here, we demonstrate the role of NMF as a small intercalant and solvent, its hydrogen-bond interactions with MXene surfaces, and its effectiveness in preventing swelling and degradation of $Ti_3C_2T_x$ MXene films [Fig. 1(a)].

$Ti_3C_2T_x$ MXene was prepared by selective etching of Al layers from Ti_3AlC_2 MAX precursor using a mixture of HF and HCl, followed by delamination of the multilayer MXene particles into single-layer MXene nanosheets through Li^+ intercalation, see Supplementary Information for detail. The pristine MXene suspension was freeze-dried and redispersed well in either water (MXene-water) or NMF (MXene-NMF), as shown in the inset of Fig. S1 for MXene-NMF. $Ti_3C_2T_x$ MXene is more chemically stable in NMF, which is a highly polar solvent, than in water, as shown by concentration measurements using UV–Vis absorption spectroscopy (Fig. S1).[23] Therefore, NMF is advantageous as a solvent for long-term storage of MXene dispersions.

The MXene-NMF dispersions can be readily used for liquid-phase processing such as spray-coating on glass substrates [Fig. 1(b)]. Structural analysis of the films using X-ray diffraction (XRD) measurements combined with thermogravimetric and mass spectrometric (TG-MS) analyses of the films scraped from the substrate, confirmed the presence of NMF between MXene layers. The TG curve for MXene-NMF shows three characteristic transformations with a weight loss of ~0.5 wt% at 100°C, ~2 wt% at 200°C, and ~1 wt% at ~330°C. The weight losses correspond well to the MS curves for the signals with $m/z = 18$ (water), $m/z = 59$ (NMF, C_2H_5NO) and $m/z = 30$ (CH_4N^+), respectively [Fig. 1(c)]. The latter fragment results from thermal decomposition of NMF during the TG-MS measurement. In comparison, the TG-MS analysis for MXene-water confirms that only water evolves from the sample in this temperature range (Fig. S3).

XRD measurements of MXene-NMF films were performed under ambient conditions to estimate the ordering and alignment of the MXene nanosheets [Fig. 1(d)]. All observed peaks can be assigned to the out-of-plane 00l reflections ($l = 2$, 4, 6…), confirming the uniform layer-by-layer stacking of MXene nanosheets parallel to the surface of the substrate. The observed c-lattice parameter was larger for MXene-NMF, 26.69(8) Å, than for MXene-water, 25 Å [Fig. 1(d) inset]. Therefore, a monolayer of intercalated water molecules[24] in the pristine sample was substituted by larger NMF molecules in the MXene-NMF. Similarly, clay minerals also showed expansion in the c-lattice parameter after intercalation of NMF.[22,25,26] Scanning electron microscopy (SEM) analysis confirmed that both pristine and functionalized MXene films showed similar ordered film structures (Figure S4). The electrical conductivity of the functionalized MXene film (4630 ± 380 S cm^{-1}) was comparable to that of the pristine film (5447 ± 670 S cm^{-1}), which were calculated based on measurements of the film thickness with a stylus profilometer (Figure S2). The conductivity values are lower than recently reported for MXene films[27] probably due to the nature of the non-stoichiometric MAX phase and freeze-dried

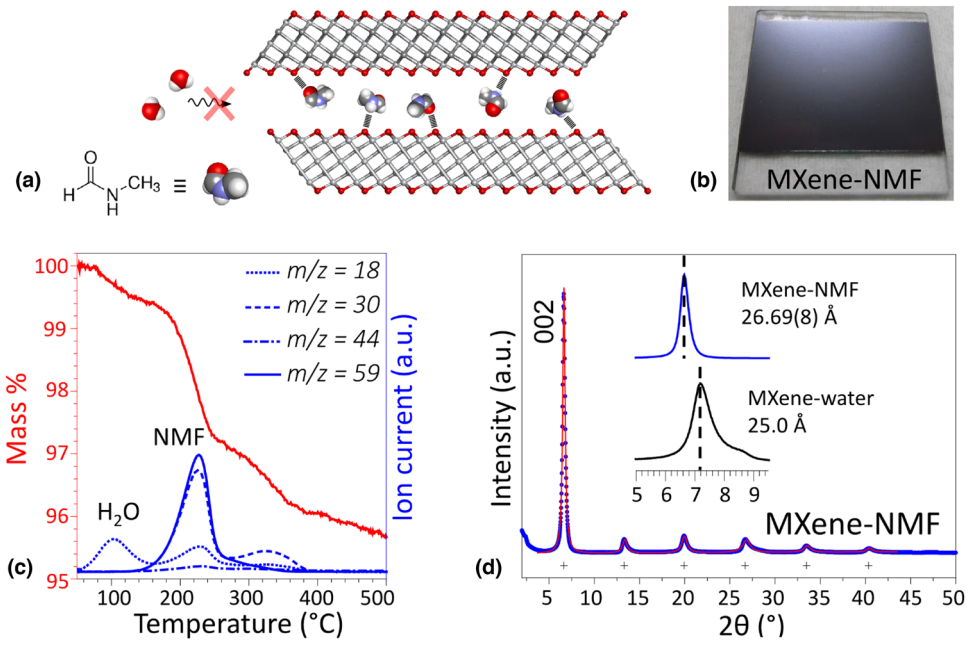

Figure 1. (a) Schematic representation of the host–guest interactions through hydrogen bonding between $Ti_3C_2T_x$ MXene and *N*-methylformamide (NMF) to improve the environmental stability of MXene films. (b) A photograph of the NMF intercalated MXene film (MXene-NMF) on a glass substrate. (c) Thermogravimetric (TG) curve and mass spectroscopy (MS) analysis of the evolved gases from MXene-NMF. (d) XRD pattern of MXene-NMF film at room temperature showing observed data (blue), fitting curve (red), and Bragg peaks (black+). The inset shows magnified XRD patterns of the 002 peaks for MXene-NMF (blue) and MXene-water (black) with the corresponding c-lattice parameter. The dashed line is a guide for the eye.

clay that were used in this study. The ~15% drop in electrical conductivity for the MXene-NMF film compared to MXene-water is attributed to the slight increase in interlayer spacing of the functionalized MXene films. In comparison, the previously used hydrogen-bonded macromolecules led to a 50% or higher decrease in electrical conductivity.[16]

Since MXene films are known to remain intact and show no morphological and minimal property changes at room temperature in laboratory air over multiple years, the prepared films were subjected to accelerated aging tests under high temperature and high humidity conditions (60°C, 85% relative humidity) for 2 weeks (Fig. 2), which are commonly used in semiconductor industry for the accelerated aging test.[28] The sheet resistance of the MXene-water film increased by 70% after one day, then stabilized at ~250% of the original value after 7 days. In comparison, the sheet resistance of the MXene-NMF film showed no significant increase after one day and a slight increase of ~44% after 7 days.

To better understand the improved environmental stability (conductivity retention) of MXene-NMF films, we studied their structural evolution during the accelerated aging tests. Figure 3(a) shows the evolution of the out-of-plane 00*l* reflections ($l = 2, 4$). The interlayer spacing of the MXene-NMF decreases over time [Fig. 3(a) and S5]. After 7 days, the shift in the 002 reflection for MXene-NMF from 6.645° to 6.817° can be attributed to partial replacement of the NMF molecules with water [Fig. 3(a)]. The interlayer spacing of the MXene-water sample was initially smaller, but, unlike MXene-NMF, it increased over time [Fig. 3(b)]. Humidity-induced lattice contraction in MXene-NMF was quantitatively confirmed by the change in the *d*-spacing of (002) plane (d_{002}) from 13.294 Å to 13.218 Å and 12.959 Å, after 1 and 7 days, respectively (Fig. S5). The presence of a mixture of intercalants (water and NMF) leads to structural inhomogeneity and broadening of the diffraction peaks during the accelerated aging test. The full width at half-maximum (FWHM) of the 002 peak increased from 0.321° initially to 0.454° after 7 days and saturated at 0.458° after 14 days. This indicates that water diffusion in the adjacent layers reached equilibrium (Fig. S5). Higher order 00*l* reflections ($l > 8$) in the XRD patterns show that the intercalants are not mixed together, but exist as distinct regions within the same film similar to interstratified MXene crystals with one or two layers of intercalated water [Fig. 3(c)]. For instance, the 0010 peak is composed of two peaks at ca. 33.5° and 35.5°, corresponding to the NMF and water-rich regions, respectively. The contribution from the NMF-rich phase decreases from 62 to 45% after 7 days, and to 41% after 14 days. These observations suggest that exposure to moisture leads to partial substitution of intercalated NMF with water. However, the residual intercalated NMF molecules are still sufficient to enhance the environmental stability of the MXene films.

In addition to swelling, degradation of $Ti_3C_2T_x$ MXenes due to oxidation and hydrolysis can contribute to decreased conductivity through MXene decomposition, increased surface metal oxidation state, and growth of TiO_2 nanocrystals.[29] To probe the surface oxidation, X-ray photoelectron spectroscopy (XPS) measurements were collected for the outermost and inner surfaces of MXene-water (Fig. S8, Table S1) and MXene-NMF (Fig. S9, Table S2) films after 7 days of accelerated aging tests. The outer surfaces of MXene-water and MXene-NMF

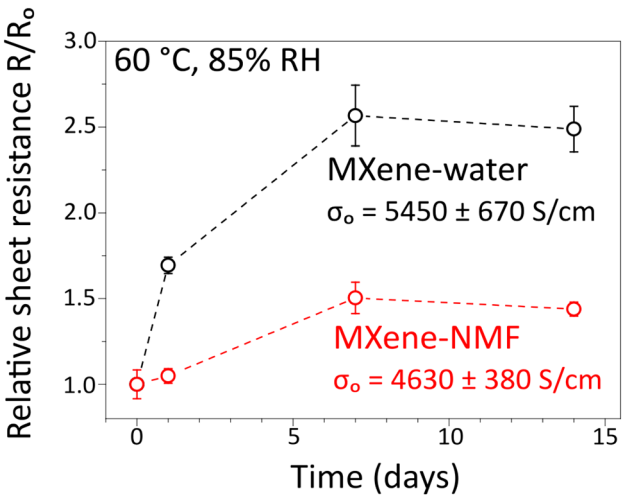

Figure 2. (a) Changes in the relative sheet resistance (R/R_0 where R_0 indicates the initial sheet resistance) of MXene-water (black) and MXene-NMF (red) films stored at 60°C and 85% RH. The initial conductivity values are also shown. Error bars denote the standard deviation.

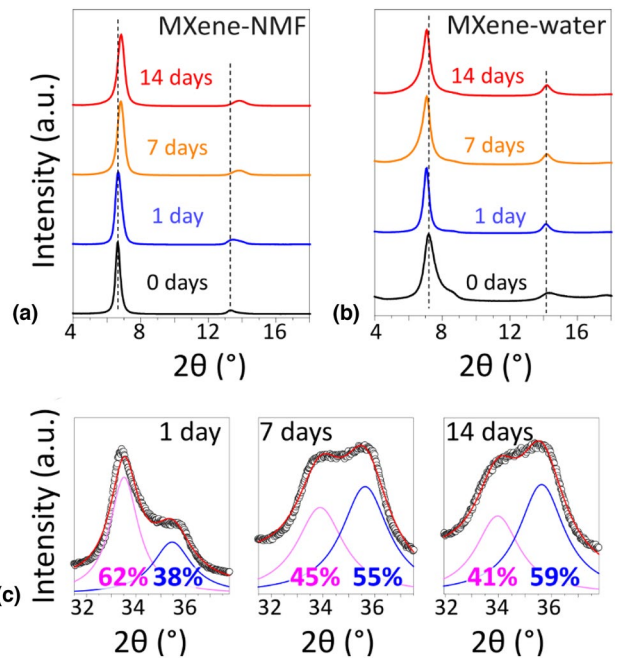

Figure 3. XRD patterns of (a) MXene-NMF and (b) MXene-water films before (0 days), and after 1, 7, and 14 days of storage at 60°C and 85% RH. (c) XRD patterns of the 0010 reflection for MXene-NMF (black) and results of peak fitting (red) after 1, 7, and 14 days. The magenta and blue component denote NMF-rich and water-rich crystalline phase, respectively. The peak area ratio is shown in each panel.

films were highly oxidized. Peak fitting of XPS spectra shows that the Ti $2p_{3/2}$ component centered at 458.9 eV (attributed to Ti^{4+} and indicative of TiO_2) contributed to more than 24% for MXene-water and 33% for MXene-NMF, with respect to the total Ti *2p* core-level spectra. In contrast, the inner surface of the MXene-NMF film was less oxidized than that of the MXene-water film, where the oxide components contributed to 2.3% (Fig. S9 and Table S2) and 6% (Fig. S8 and Table S1), to the total Ti *2p* core-level spectra, respectively.

The improved stability of MXene-NMF can be attributed to two mechanisms. (i) NMF molecules, by occupying the space in between the layers or by bridging two adjacent MXene layers, can suppress diffusion of water and prevent it from intercalating deeper into the film, similar to the previously studied hydrazine molecules[20]. (ii) NMF molecules can bond to the surface termination groups of MXene through hydrogen bonding and prevent water molecules from starting oxidation reactions. In particular, the Ti–OH site is sensitive to oxidation.[4] Deprotonation of the Ti–OH group, coupled with the formation of a protective solvent cage, helps to stabilize MXene against degradation.[30] Similarly, the carbonyl oxygen in NMF could act as a hydrogen acceptor to form hydrogen bond with hydroxyl surface terminations, thus, sterically protecting this active site from water.

To support the proposed protection mechanisms, we performed first-principles calculations on the geometry of the NMF molecules between MXene sheets [Fig. 4(a)]. Since the concentration of NMF in the MXene-NMF sample is low, ~3 wt% from TG measurements, self-interaction between NMF molecules can be ignored within the simulation. The surfaces of MXene synthesized were functionalized with –O, –OH, –F, and –Cl termination groups, as confirmed by combustion ion chromatography (see Materials and Methods). Therefore, structural optimization was performed by modeling the mixed surface termination as $Ti_3C_2F_{0.875}Cl_{0.125}(OH)_{0.125}O_{0.875}$ with intercalated *trans*-NMF molecules. In the initial structure, both O–H(MXene)···O=C(NMF) and O(MXene)···H–N(NMF) were set to ~2 Å, so that the intercalated system could offer the formation of dual hydrogen bonds. The distance between MXene layers was set to 13.35 Å, corresponding to the experimental value measured with XRD. Interestingly, the NMF molecules in the optimized structure were oriented parallel to the MXene surface with the carbonyl group close to the surface and H–N of the amide group away from the surface. The length of the O–H(MXene)···O=C(NMF) bond was 1.60 Å [Fig. 4(b)], indicating that the intercalant was accommodated between the layers via hydrogen bonding. These results suggest that the preferred adsorption site for NMF is –OH rather than –O surface termination group, and the adsorption energy in this geometry was estimated to be −0.947 eV.

We also carried out calculations to investigate the proton-donating ability of NMF using MXenes with a uniform surface termination composition (–O and –F, Figs. S10 and S11). For MXene terminated with –O groups, the hydrogen atoms in the amide group were close to the terminations and the O(MXene)···H–N(NMF) bond length was 2.07 Å. The adsorption energy was estimated to be −0.113 eV, comparable to that of water, −0.109 eV (Fig. S12). In contrast, for the -F–terminated MXene, the NMF molecules were oriented parallel to the surface (Fig. S11), and the F(MXene)···H–N(NMF) bond length was 3 Å. The larger F–H bond length compared to O–H bond suggests that F-terminations are less thermodynamically favorable to interact with NMF. Finally, the differential charge density plot illustrates the formation of a hydrogen bond between -OH termination and NMF, as shown by the charge density gain near the oxygen of the NMF molecule and charge density loss near the hydrogen of the -OH termination [Fig. 4(c)]. Overall, our calculations suggest that NMF strongly interacts with -OH terminations and protects these sites from oxidative degradation.

In conclusion, the stability of $Ti_3C_2T_x$ MXene films in environments with high humidity and elevated temperatures can be significantly improved by intercalation of *N*-methylformamide, which strongly interacts with the MXene surface through hydrogen bonding. Intercalation of NMF between MXene nanosheets and their interactions were confirmed through structural and physical characterization of the films and theoretical calculations. NMF effectively mitigates swelling of MXene

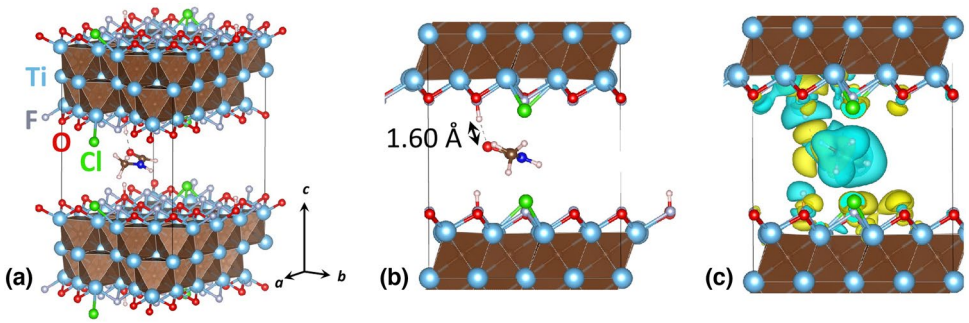

Figure 4. (a) Perspective view of the optimized structure of $Ti_3C_2T_x$ MXene with a mixture of –O, –OH, and –F surface terminations and an intercalated NMF molecule; and (b, c) as viewed along the [100] direction. The interlayer spacing was set to an experimentally measured value of 13.35 Å based on XRD results in Fig. 1(d). The length of the O–H(MXene)···O(NMF) bond is approximately 1.60 Å. (c) The differential charge density plot of the optimized structure, describing the charge gain (yellow) and loss (blue) after NMF intercalation.

films through capture of water from moisture in the air, thus slowing down the oxidation and hydrolysis reactions that would lead to degradation. As a result, the functionalized MXenes films exhibited a smaller increase in the electrical conductivity of less than ~ 50% compared to the pristine MXene films which exhibited an ~ 150% increase, after storage for 2 weeks at 60°C and 85% relative humidity. This study suggests that intercalation of small molecules that can strongly interact with MXenes via hydrogen bonding may provide an easy path to improving the stability of MXene films and coatings intended for use under high humidity and high temperature conditions, such as in tropical climates and some industrial environments.

Acknowledgments

This work was supported by Murata Manufacturing Co., Ltd., Japan.

Declarations

Conflict of interest

The authors declare no competing financial interest.

Supplementary Information

The online version contains supplementary material available at https://doi.org/10.1557/s43579-023-00350-5.

References

1. A. VahidMohammadi, J. Rosen, Y. Gogotsi, The world of two-dimensional carbides and nitrides (MXenes). Science **372**, 6547 (2021). https://doi.org/10.1126/science.abf1581
2. B. Anasori, Y. Gogotsi, *2D Metal carbides and nitrides (MXenes): structure properties and applications* (Springer Cham, Gewerbestr, 2019)
3. A. Iqbal, J. Hong, T.Y. Ko, C.M. Koo, Improving oxidation stability of 2D MXenes: synthesis, storage media, and conditions. Nano. Converg. **8**, 9 (2021). https://doi.org/10.1186/s40580-021-00259-6
4. F. Xia, J. Lao, R. Yu, X. Sang, J. Luo, Y. Li, J. Wu, Ambient oxidation of Ti_3C_2 MXene initialized by atomic defects. Nanoscale **11**, 23330 (2019). https://doi.org/10.1039/C9NR07236E
5. S. Huang, V.N. Mochalin, Understanding chemistry of two-dimensional transition metal carbides and carbonitrides (MXenes) with gas analysis. ACS Nano. **14**, 10251 (2020). https://doi.org/10.1021/acsnano.0c03602
6. E.S. Boek, P.V. Coveney, N.T. Skipper, Monte carlo molecular modeling studies of hydrated Li-, Na-, and K-smectites: understanding the role of potassium as a clay swelling inhibitor. J. Am. Chem. Soc. **117**, 12608 (1995). https://doi.org/10.1021/ja00155a025
7. C.A. Voigt, M. Ghidiu, V. Natu, M.W. Barsoum, Anion adsorption, $Ti_3C_2T_z$ MXene multilayers, and their effect on claylike swelling. J. Phys. Chem. C **122**, 23172 (2018). https://doi.org/10.1021/acs.jpcc.8b07447
8. J.L. Hart, K. Hantanasirisakul, A.C. Lang, B. Anasori, D. Pinto, Y. Pivak, J.T. van Omme, S.J. May, Y. Gogotsi, M.L. Taheri, Control of MXenes' electronic properties through termination and intercalation. Nat. Commun. **10**, 522 (2019). https://doi.org/10.1038/s41467-018-08169-8
9. J. Halim, E.J. Moon, P. Eklund, J. Rosen, M.W. Barsoum, T. Ouisse, Variable range hopping and thermally activated transport in molybdenum-based MXenes. Phys. Rev B **98**, 104202 (2018). https://doi.org/10.1103/PhysRevB.98.104202
10. H.J. Koh, S.J. Kim, K. Maleski, S.Y. Cho, Y.J. Kim, C.W. Ahn, Y. Gogotsi, H.T. Jung, Enhanced Selectivity of MXene gas sensors through metal ion intercalation: in situ X-ray diffraction study. ACS Sens. **4**, 1365 (2019). https://doi.org/10.1021/acssensors.9b00310
11. L. Ding, L. Li, Y. Liu, Y. Wu, Z. Lu, J. Deng, Y. Wei, J. Caro, H. Wang, Effective ion sieving With $Ti_3C_2T_x$ MXene membranes for production of drinking water from seawater. Nat. Sustain. **3**, 296 (2020). https://doi.org/10.1038/s41893-020-0474-0
12. R. Bian, S. Xiang, D. Cai, Fast treatment of MXene films with isocyanate to give enhanced stability. ChemNanoMat **6**, 64 (2020). https://doi.org/10.1002/cnma.201900602
13. H. Zhou, S.J. Han, H.-D. Lee, D. Zhang, M. Anayee, S.H. Jo, Y. Gogotsi, T.-W. Lee, Overcoming the limitations of MXene electrodes for solution-processed optoelectronic devices. Adv. Mater. **34**, 2206377 (2022). https://doi.org/10.1002/adma.202206377
14. S. Wan, X. Li, Y. Chen, N. Liu, Y. Du, S. Dou, L. Jiang, Q. Cheng, High-strength scalable MXene films through bridging-induced densification. Science **374**, 96 (2021). https://doi.org/10.1126/science.abg2026
15. Z. Lu, Y. Wei, J. Deng, L. Ding, Z.-K. Li, H. Wang, Self-Crosslinked MXene ($Ti_3C_2T_x$) membranes with good antiswelling property for monovalent metal ion exclusion. ACS Nano. **13**, 10535 (2019). https://doi.org/10.1021/acsnano.9b04612
16. Z. Hao, S. Zhang, S. Yang, X. Li, Y. Gao, J. Peng, L. Li, L. Bao, X. Li, Bridged $Ti_3C_2T_x$ MXene film with superior oxidation resistance and structural stability for high-performance flexible supercapacitors. ACS Appl. Energy. Mater. **5**, 2898 (2022). https://doi.org/10.1021/acsaem.1c03575
17. S. Tu, Q. Jiang, X. Zhang, H.N. Alshareef, Large dielectric constant enhancement in mxene percolative polymer composites. ACS Nano **12**, 3369 (2018). https://doi.org/10.1021/acsnano.7b08895
18. W.-T. Cao, F.-F. Chen, Y.-J. Zhu, Y.-G. Zhang, Y.-Y. Jiang, M.-G. Ma, F. Chen, Binary strengthening and toughening of MXene/cellulose nanofiber composite paper with nacre-inspired structure and superior electromagnetic interference shielding properties. ACS Nano. **12**, 4583 (2018). https://doi.org/10.1021/acsnano.8b00997
19. Y.-Z. Zhang, J.K. El-Demellawi, Q. Jiang, G. Ge, H. Liang, K. Lee, X. Dong, H.N. Alshareef, MXene hydrogels: fundamentals and applications. Chem. Soc. Rev. **49**, 7229 (2020). https://doi.org/10.1039/D0CS00022A
20. O. Mashtalir, M.R. Lukatskaya, A.I. Kolesnikov, E. Raymundo-Pinero, M. Naguib, M.W. Barsoum, Y. Gogotsi, The effect of hydrazine intercalation on the structure and capacitance of 2D titanium carbide (MXene). Nanoscale **8**, 9128 (2016). https://doi.org/10.1039/c6nr01462c
21. H. Tan, W. Qu, G. Chen, R. Liu, The role of charge transfer in the hydrogen bond cooperative effect of *cis*-N-methylformamide oligomers. J. Phys. Chem. A **109**, 6303 (2005). https://doi.org/10.1021/jp051444q
22. B. Caglar, B. Afsin, E. Eren, A. Tabak, C. Cirak, O. Cubuk, The spectral, structural and thermal characterizations of dimethyl sulphoxide, pyridine, ethanol-amine and N-methyl formamide intercalated kaolinites. Zeitschrift für Naturforschung A **65**, 1009 (2010). https://doi.org/10.1515/zna-2010-1111
23. K. Maleski, V.N. Mochalin, Y. Gogotsi, Dispersions of two-dimensional titanium carbide MXene in organic solvents. Chem. Mater. **29**, 1632 (2017). https://doi.org/10.1021/acs.chemmater.6b04830
24. M. Ghidiu, J. Halim, S. Kota, D. Bish, Y. Gogotsi, M.W. Barsoum, Ion-exchange and cation solvation reactions in Ti_3C_2 MXene. Chem. Mater. **28**, 3507 (2016). https://doi.org/10.1021/acs.chemmater.6b01275
25. B.P. Kelleher, D. Sutton, T.F. O'Dwyer, The effect of kaolinite intercalation on the structural arrangements of *N*-methylformamide and 1-methyl-2-pyrrolidone. J. Colloid Interface Sci. **255**, 219 (2002). https://doi.org/10.1006/jcis.2002.8666
26. F.T. Andreou, B. Barylska, Z. Ciesielska, M. Szczerba, A. Derkowski, V. Gionis, E. Siranidi, G.D. Chryssikos, Intercalation of N-methylformamide in Kaolinite: in situ monitoring by near-infrared spectroscopy and X-ray diffraction. Appl. Clay Sci. **212**, 106209 (2021). https://doi.org/10.1016/j.clay.2021.106209
27. T.S. Mathis, K. Maleski, A. Goad, A. Sarycheva, M. Anayee, A.C. Foucher, K. Hantanasirisakul, C.E. Shuck, E.A. Stach, Y. Gogotsi, Modified MAX phase synthesis for environmentally stable and highly conductive Ti_3C_2 MXene. ACS Nano. **15**, 6420 (2021). https://doi.org/10.1021/acsnano.0c08357

28. O. Haillant, Accelerated weathering testing principles to estimate the service life of organic PV modules. Sol. Energy Mater. Sol. Cells **95**, 1284 (2011). https://doi.org/10.1016/j.solmat.2010.08.033
29. Y. Lee, S.J. Kim, Y.-J. Kim, Y. Lim, Y. Chae, B.-J. Lee, Y.-T. Kim, H. Han, Y. Gogotsi, C.W. Ahn, Oxidation-resistant titanium carbide mxene films. J. Mater. Chem. A **8**, 573 (2020). https://doi.org/10.1039/C9TA07036B
30. S. Doo, A. Chae, D. Kim, T. Oh, T.Y. Ko, S.J. Kim, D.-Y. Koh, C.M. Koo, Mechanism and kinetics of oxidation reaction of aqueous $Ti_3C_2T_x$ suspensions at different pHs and temperatures. ACS Appl. Mater. Inter. **13**, 22855 (2021). https://doi.org/10.1021/acsami.1c04663